

Multi-Frame MQD-PIV

Yong Kweon Suh*

*School of Mechanical and Industrial System Engineering, Dong-A University,
840 Hadan-dong, Saha-gu, Busan 604-714, Korea*

In this paper, we propose a new PIV methodology for obtaining a velocity field from a sequence of multiple image data based on a least-square principle (also known as MQD; minimum quadratic difference) for the grey level difference between two neighboring frames of image data. We investigated both the accuracy of the result and the time consumption in the computation. It turns out that the proposed method is not only accurate but fast compared with the conventional correlation PIV techniques. Our method is applied to the spin-up flows and the results show that the method can be a good substitution for the conventional algorithms employed in the existing commercial codes.

Key Words : MQD (Minimum Quadratic Difference) PIV, Least-Square Principle, Multi-Frame PIV, Cross-Correlation, Spin-Up Flow

1. Introduction

The particle image velocimetry (PIV) has been widely used in quantitatively obtaining velocity fields from visualized images of flow fields. A practical guide to the PIV principle and processing can be found e.g. in Raffel et. al. (1998) among others. Most recently, interests are given to development of 3-D PIV (Lecerf et. al., 1999; Liu et. al., 2000) and application to MEMS (Microelectronic Mechanical System, Meinhart et. al., 1999; Beebe et. al., 2001; Strook et. al., 2002). Development of a low-cost miniature PIV system (Chetelat et al., 2001) also deserves attentions from the industrial field. On the other hand emergence of powerful computers has made the fluid dynamicist to have in mind to establish a real-time measurement of the velocity field for use in flow control. In this case, however, in parallel with the hardware improvement, the computa-

tional accuracy as well as the speed of PIV algorithms must also be increased.

Most algorithms used for detecting the displacement vector for the set of image frames to be used in calculation of the velocity vector are based on the cross-correlation method. The simple cross-correlation algorithm is preferred in that it is easy to implement and needs smaller computational effort. However it turns out that it produces substantial errors due to the reason to be explained in this paper. The normalized cross-correlation algorithm partially overcomes such shortcomings, but it needs more computational time.

In this paper we propose a new algorithm, that is, a multi-frame MQD-PIV method which is both simple in implementation and fast in operation. The MQD (Minimum Quadratic Difference) method has been initially proposed by Gui and Merzkirch (1996). The method is based on the least-square principle. In this method, the object function of an interrogation base window for a candidate interrogation search window is given by summing all the quadratic difference between the grey levels of two image sets. The particle located at the center of the base window is then assumed to arrive at the center of the search window where the object function becomes mini-

* E-mail : yksuh@mail.donga.ac.kr

TEL : +82-51-200-7648; FAX : +82-51-200-7656

School of Mechanical and Industrial System Engineering, Dong-A University, 840 Hadan-dong, Saha-gu, Busan 604-714, Korea. (Manuscript Received January 17, 2003; Revised June 13, 2003)

mum over the whole searching area of the flow field. Gui and Merzkirch (2000) conducted a comparative study of the MQD method and showed that the method is indeed more accurate than the correlation-based PIV methods. They also showed that the method can be complemented by the FFT method so that the computational speed can be kept almost the same level as the correlation-based FFT algorithm. In this paper, we show that the capability of the MQD method is further increased by employing the multi-frame method.

This paper is organized as follows. In the following section the basic idea of the simple cross-correlation and normalized cross-correlation methods are explained. It then leads to the description of the simple MQD and multi-frame MQD methods. In the section 3, we show the results of application of the various methods to a standard image set provided by the Visualization Society of Japan (VSJ). In the section 4, the methods are applied to the real images taken from the experiment of spin-up flows inside a rectangular container. The important findings of this study are then summarized in the final section.

2. Particle Image Interrogation

2.1 Simple cross-correlation method

Conventional PIV systems in most cases use the auto-correlation or cross-correlation methods in finding the particles' displacements. This method basically utilizes two consecutive images, taken at t and $t + \Delta t$ for a small time interval Δt . Figure 1 shows arrangement of windows for searching particles' paths for the time elapse Δt . In this figure, the image of the interrogation base window is given at the base time t , while that at the interrogation search window is given at the later time $t + \Delta t$.

Let's denote the intensity of the image at t and $t + \Delta t$ by $I(i, j)$ and $I'(i, j)$ respectively, where the indices i and j span over the whole pixels in the images. Then we can define the correlation (object) function S for the base window at (i, j) as

$$S(\alpha, \beta) = \sum_{a=-p}^p \sum_{b=-p}^p I(i+a, j+b) I'(i+a+\alpha, j+b+\beta) \quad (1)$$

where dependence of S on i and j is not explicitly denoted for brevity. The indices α and β span over the whole searching area, $-n_{sb} \leq \alpha, \beta \leq n_{sb}$, see Fig. 1, and p is given by

$$p = \frac{1}{2}(n_{pw} - 1) \quad (2)$$

The fluid particle situated initially at the center grid point of Fig. 1 is then supposed as a first approximation to arrive at the point (i_0, j_0) at which the function S becomes *maximum* within the searching area. To improve the sub-pixel accuracy, we may use a quadratic interpolation scheme to find a more accurate set of coordinates (i_c, j_c) . For instance i_c is given by

$$i_c = i_0 + \frac{S(i_0 - 1, j_0) - S(i_0 + 1, j_0)}{2[S(i_0 - 1, j_0) + S(i_0 + 1, j_0) - 2S(i_0, j_0)]} \quad (3)$$

Similar formulation holds for j_c . Note that i_c and j_c are not integers.

One of the most important parameters in the computations is n_{pw} which represents the size of

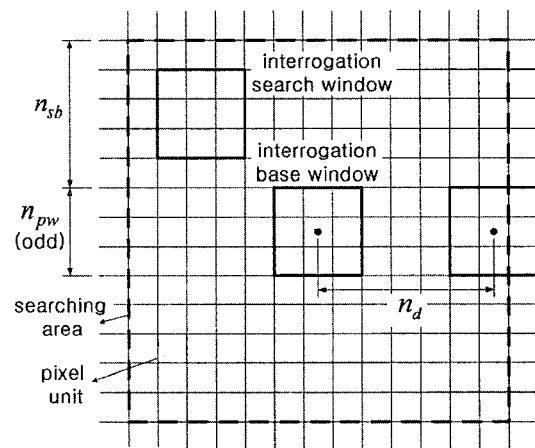


Fig. 1 Interrogation windows (surrounded by solid lines) for finding fluid particles' movement during a small interval of time Δt within a searching area (surrounded by dashed lines) for a grid point, which is shown as a dot at the center. Also shown on the right-hand side is a neighboring grid point and its base window. The pixel unit is shown as hatched

the interrogation window in the pixel unit. This value should be as small as possible, because otherwise the small-scale flows could not be properly resolved. On the other hand, the general tendency is that the number of error vectors increase as this value is decreased. The proper value of this variable depends on the particle size and the particle distribution.

Another important parameter is n_{sb} , the extent of the searching area in the pixel unit. This parameter should also be optimized. If the local fluid velocity is V and the physical length of the unit pixel Δx , this value should be larger than $V\Delta t/\Delta x$. However, if this value is taken too large, deformation of the interrogation windows will be large and we may encounter difficulty in finding the particle's displacement.

If the total number of grid points along the x -direction, at which the velocity vectors are defined, is denoted by N_w , the distance in the pixel unit between the neighboring grids n_d (see Fig. 1) is computed by

$$n_d = \text{int} \left[\frac{i_m - 2(n_{sb} + p)}{N_w} \right] \quad (4)$$

where i_m is the total number of pixels along the x -direction. Similar formulation holds for n_d along the y -direction. The velocity components are then given by

$$u = \frac{(i_c - i)\Delta x}{\Delta t}, \quad v = \frac{(j_c - j)\Delta x}{\Delta t} \quad (5)$$

2.2 Normalized cross-correlation method

The simple cross-correlation method described in the previous section can be implemented by normalization. The correlation function in this case takes the form

$$S(\alpha, \beta) = \frac{\sum_{a=-pb}^p \sum_{b=-p}^p [I(i+a, j+b) - \bar{I}(i, j)][I'(i+a+a, j+b+\beta) - \bar{I}'(i+a, j+\beta)]}{\mu(i, j)\mu'(i+a, j+\beta)} \quad (6)$$

where \bar{I} and \bar{I}' are the averages and μ and μ' are the variances of the intensities I and I' , respectively;

$$\begin{aligned} \bar{I}(i, j) &= \sum_{a=-pb}^p \sum_{b=-p}^p I(i+a, j+b), \\ \bar{I}'(i+a, j+\beta) &= \sum_{a=-pb}^p \sum_{b=-p}^p I'(i+a+a, j+b+\beta), \\ \mu(i, j) &= \sqrt{\sum_{a=-pb}^p \sum_{b=-p}^p [I(i+a, j+b) - \bar{I}(i, j)]^2}, \\ \mu'(i+a, j+\beta) &= \sqrt{\sum_{a=-pb}^p \sum_{b=-p}^p [I'(i+a+a, j+b+\beta) - \bar{I}'(i+a, j+\beta)]^2} \end{aligned}$$

2.3 Simple MQD method

With the MQD method, instead of using the correlation function (1) or (6), we use the function

$$S(\alpha, \beta) = \sum_{a=-pb}^p \sum_{b=-p}^p [I(i+a, j+b) - I'(i+a+a, j+b+\beta)]^2 \quad (7)$$

and find the point (i_0, j_0) at which the function S becomes *minimum* within the searching area. The algorithm to find an improved set of points (i_c, j_c) is the same as equation (3).

2.4 Multi-frame MQD method

In most cases, some of particles situated initially within the volume of narrow light sheet escape the volume at a later time, and simultaneously particles situated initially out of the volume enter the domain. This happening clearly deteriorates the computed velocity field and serves as one of the primary reasons for error vectors. Another factor influencing the accuracy of the computation may be particles' adherence to or detachment from each other during the time interval Δt making the image pattern change instantaneously. In the following discussions, these happenings are referred to as "pattern deterioration".

The error vectors caused by these can be partially removed if we use multiple frames in identifying the locus of fluid particles. For instance, in the four-frame method, let the function S_1, S_2, S_3 , denote the evaluation of equation (7) for the pair of frames (1st, 2nd), (2nd, 3rd), and (3rd, 4th), respectively. Then we compute the averaged ones by

$$S(\alpha, \beta) = S_1(\alpha, \beta) + S_2(\alpha, \beta) + S_3(\alpha, \beta) \quad (8)$$

and search the point (i_0, j_0) at which the function S becomes *minimum*. The subsequent procedure

is the same as previously stated.

When there are no pattern deteriorations in the three pairs, the velocity data obtained by the multi-frame method represent the temporally averaged ones at $t + 3\Delta t/2$; note that, for example, the two-frame method for the pair (1st, 2nd) images yields the velocity field at $t + \Delta t/2$. When there is a pattern deterioration for the pair e.g. (1st, 2nd), the velocity data given by the four-frame method represent the ones at $t + 2\Delta t$, and so on.

3. Results of Application to the Standard Images

Figure 2 shows an example of image set taken from VSJ standard images (<http://www.vsj.or.jp/indexe.html>). For further analysis in a FORTRAN routine, these image files are then converted into a ASCII format by using a MATLAB m-function.

In this code four images are first converted into double-precision data sets so that they can be algebraically processed. The four images are then superposed so that the result represent pathlines of the flow field subjected to this image process; the data is apriori transformed into uint 8 data type so that they can be plotted in a figure frame as shown in Fig. 3.

Figure 4 shows the velocity vectors obtained by applying the simple cross-correlation method to the two standard images, (a) and (b) of Fig. 2. In

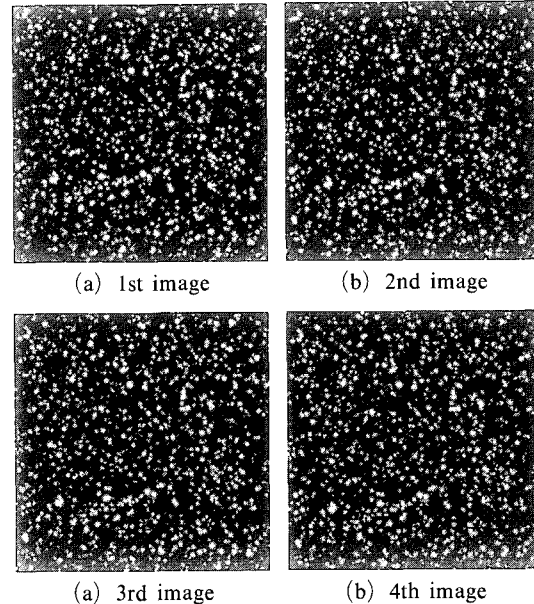


Fig. 2 A set of standard images named '2D jet flow' with 256×256 pixels taken from the home page of Visualization Society of Japan

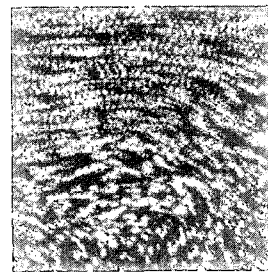


Fig. 3 Pathlines made by superposition of the four images shown in Fig. 2

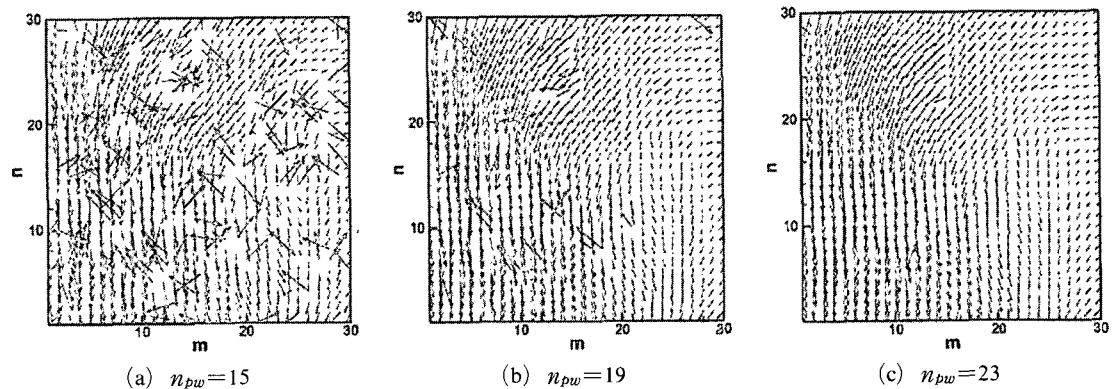


Fig. 4 Velocity vectors obtained by applying the simple cross-correlation method to the (1st, 2nd) image set of Fig. 2 for $n_{sb}=7$

this computation, the parameter n_{sb} is fixed as 7. The indices m and n denote the grid at which a specific interrogation base window is situated for the velocity computation. In this figure, total 30×30 velocity vectors are shown in each frame. It is shown expectedly that the accuracy is improved as n_{pw} is increased, and we need at least $n_{pw}=23$ for a reasonable result.

Figure 5 shows the results when the normalized cross-correlation method is applied to the same image set. We can see that the vector-field pattern is much smoother than that of Fig. 4 at the same value of n_{pw} . This clearly indicates that the normalized cross-correlation algorithm provides much better results than the simple cross-correlation method. However in this case we could not obtain the results when n_{pw} is less than 11

because the variance μ' becomes zero at certain base or search windows. This becomes a serious drawback especially when particles are sparsely distributed.

Figure 6 shows the results when the simple MQD method is applied to the same image set. It is seen that this method yields almost the same accuracy as the cross-correlation method at the same n_{sb} . However in this method no problems have been encountered at low n_{pw} values.

The PIV measurement of the velocity vector is further improved when the multi-frame MQD method is used. Figure 7 shows the velocity vectors given by three methods for $n_{sb}=7$ and $n_{pw}=9$. In this figure, for a clearer view, the indices along the n -direction are periodically skipped. It exhibits that the four-frame MQD method gives

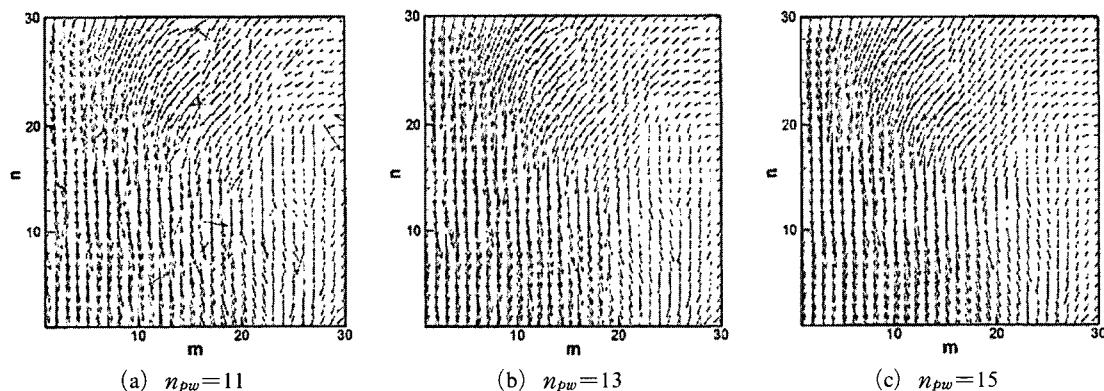


Fig. 5 Velocity vectors obtained by applying the normalized cross-correlation method to the (1st, 2nd) image set of Fig. 2 for $n_{sb}=7$

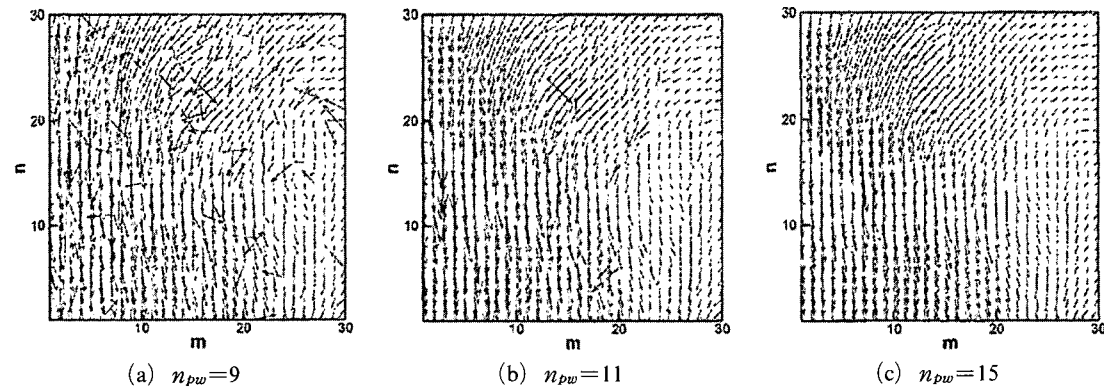


Fig. 6 Velocity vectors obtained by applying the 2-frame MQD method to the same image set of Fig. 4 for $n_{sb}=7$

the best result.

The reason why the MQD methods (and similarly the normalized c-c methods) provide better results compared with the simple c-c methods can be explained in details. It is seen from Fig. 7 that the simple c-c method (Fig. 7(a)) gives an error vector at the grid point $(m, n) = (12, 28)$, whereas the simple MQD method gives a correct one (Fig. 7(b)). So, we focus on this local area to

dignify the reason. Figure 8 shows distributions of the function S obtained by the two methods for the grid point $(m, n) = (12, 28)$.

In Fig. 8(a) the function S has several local peaks. However, the highest peak is not at the true point, indicated by a dashed arrow, but at an erroneous point, indicated by a solid arrow. On the other hand, the function S has also several humps in Fig. 8(b), but in this case the lowest

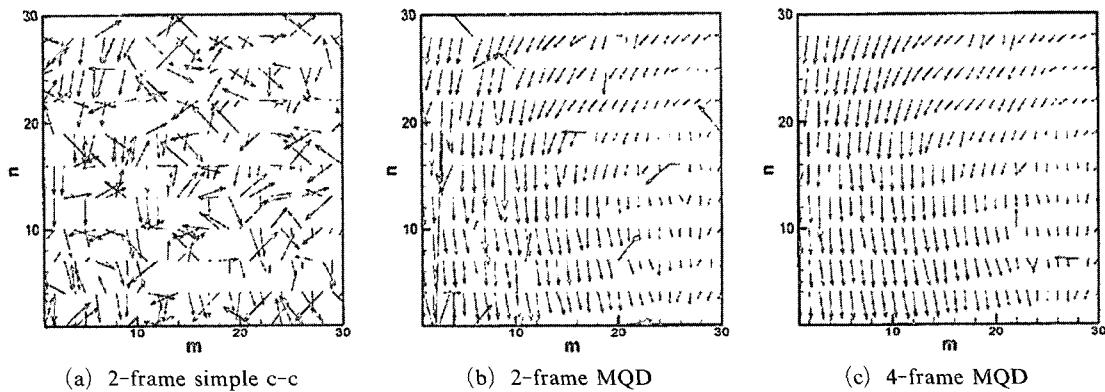


Fig. 7 Velocity vectors given by the simple cross-correlation and the MQD methods to the standard images of Fig. 2 for $n_{sb}=7$ and $n_{pw}=9$

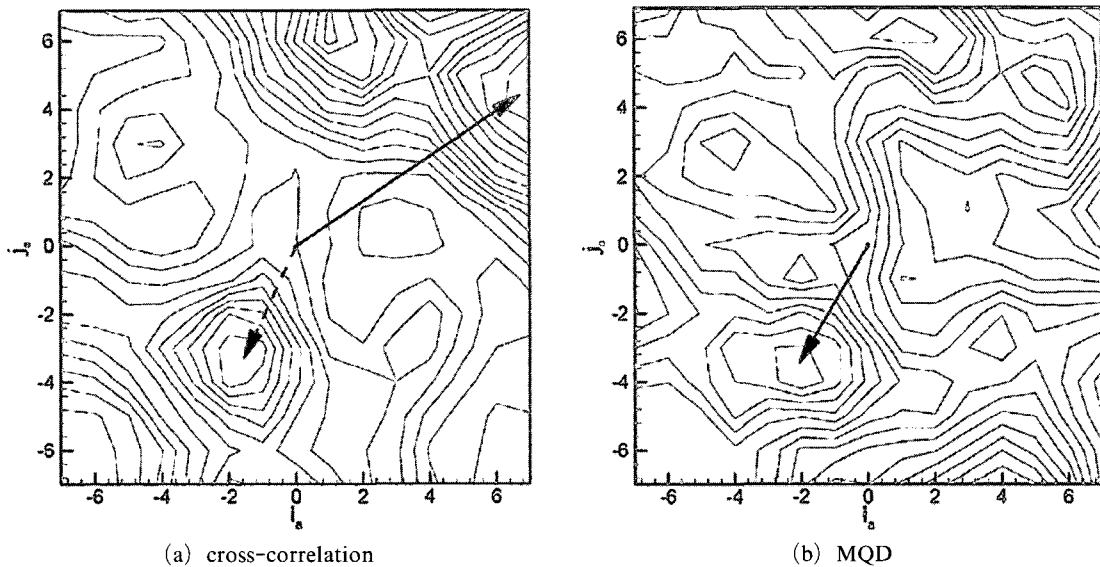


Fig. 8 Distributions of the function S given by the (a) cross-correlation without normalization and (b) MQD methods. The solid vector in each frame corresponds to the pattern's displacement which is parallel to the velocity vector to be obtained ; in (a) the vector is classified as "error vector" whereas in (b) it is correct. The dashed vector in (a) indicates the correct one but not detected in the simple cross-correlation method

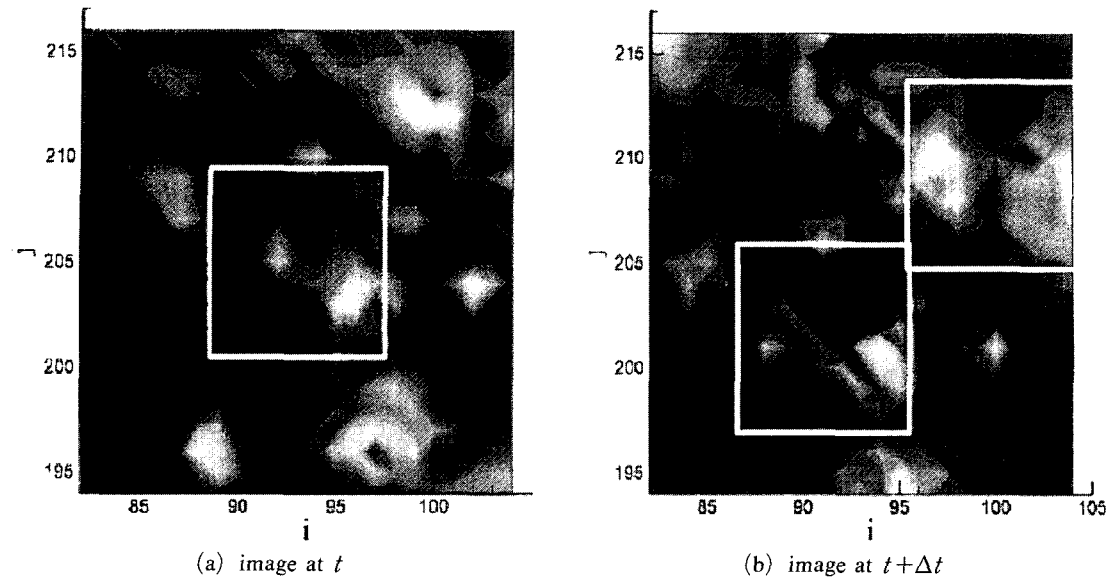


Fig. 9 Interrogation windows within a searching area in the two sequential images. The central window in (a) is the interrogation base window, the one on the right-hand side in (b) the search window which yields a maximum of S in the cross-correlation method, and the one the bottom in (b) the search window which yields a minimum of S in the MQD method

hump is at the true point, indicated by a solid arrow.

The reason for the occurrence of the error vector in the conventional method can be explained in terms of the distributions of the pattern intensity at two sequential instants as shown in Fig. 9. The center point of this figure coincides with that of Fig. 8. In this figure the base window (grey one in (a)) couples with the white window in (b) to give the maximum of S in the simple c-c method, while it couples with the grey window to give the minimum of S in the MQD method. It clearly indicates that the MQD method predicts well the true pattern movement, whereas the simple c-c method predicts it erroneously.

The reason for the maximum of S at the erroneous point in the simple c-c method is evident. The interrogation window on the right-hand side in Fig. 9(b) ('9br' hereafter) is covered with high intensity values of I' . When this is correlated with the intensity I of the base window in (a), it results in S which is bigger than when the base window of (a) is correlated with the one near the bottom in (b) ('9bt' hereafter), because the broad area of 9br is characterized by a high intensity value. As

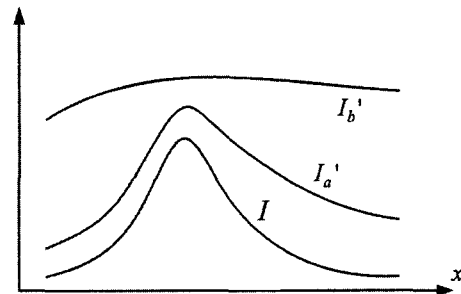
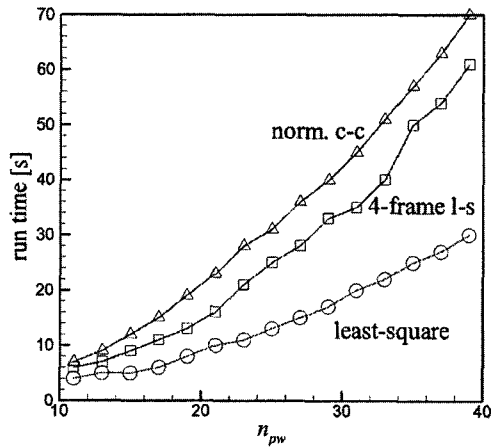
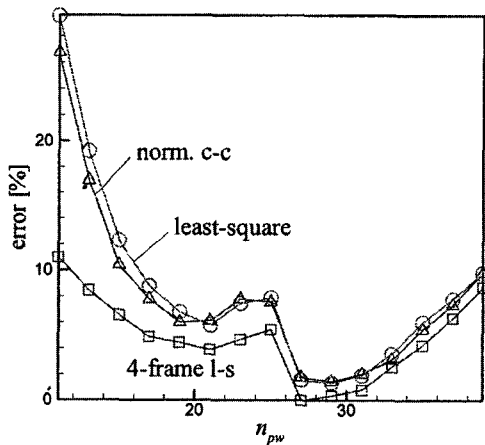
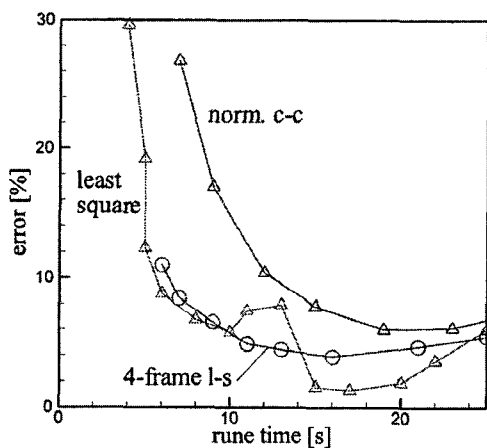


Fig. 10 Examples of intensity distributions of the search window, I_a' and I_b' and that of the base window, I

a distinct case, when the whole pixels of 9br are given with a highest intensity (that is, the image colored white), the simple c-c method always predicts the center point of 9br as the displaced position of the center of the base window in (a), which is clearly erroneous.

Figure 10 shows two examples of intensity function, I_a' and I_b' of interrogation search windows and an intensity function I of the base window, all the functions being given as one-dimensional for simplicity. In this case the intensity I_a' is in overall less than the intensity I_b' but it is closer

(a) Run time versus n_{pw} (b) Error versus n_{pw} 

(c) Error versus run time

Fig. 11 Comparison of run times [s] and error [%] obtained by three PIV methods for the standard images named '3-D impingement/reference' given by VSJ

to I , and therefore it should be selected as a correct pattern resembling the original intensity field I . However, the functional value of S in the correlation between I and I_a' will be smaller than that between I and I_b' , which is not preferable. However the value of S in the MQD method becomes smaller for the coupling $I-I_a'$, than for the coupling $I-I_b'$, which is reasonable.

To evaluate the performance of each method the run time of the code and error of the results each method yields must be compared. For this, the standard images for a three-dimensional impingement flow given by VSJ have been used. In the estimation of the error we used the PIV result given by the four-frame MQD method with $n_{sb}=11$ and $n_{pw}=27$ as a basis. The error percentage represents the ratio of the number of error vectors and the total number of vectors in the field, which is 900. The error vector is defined as the one which differs from the basis as much as 20% in magnitude, relative to the largest one in the field.

Figure 11 shows the results. As shown in Fig. 11(a), the run time for the normalized c-c method is more than twice that of the simple MQD method for the same n_{pw} . It is also remarkable that the 4-frame MQD method is even faster than the c-c method. On the other hand the error level of the simple MQD method is slightly higher than the c-c method, see Fig. 11(b). The reason that all the methods provide the minimum error near $n_{pw}=27$ is due to the fact that the basis data is generated at $n_{pw}=27$. In the economical point of view, the error level must be compared at the same run time, as shown in Fig. 11(c). It reveals that the simple MQD and 4-frame MQD methods being almost in the same performance are better than the 2-frame (simple) c-c method.

4. Results of Application to the Spin-up Flows Inside a Rectangular Container

The present methods are applied to the spin-up flow inside a rectangular container with the horizontal dimensions 40 cm \times 20 cm and liquid depth 11.8 cm. The numerical and experimental

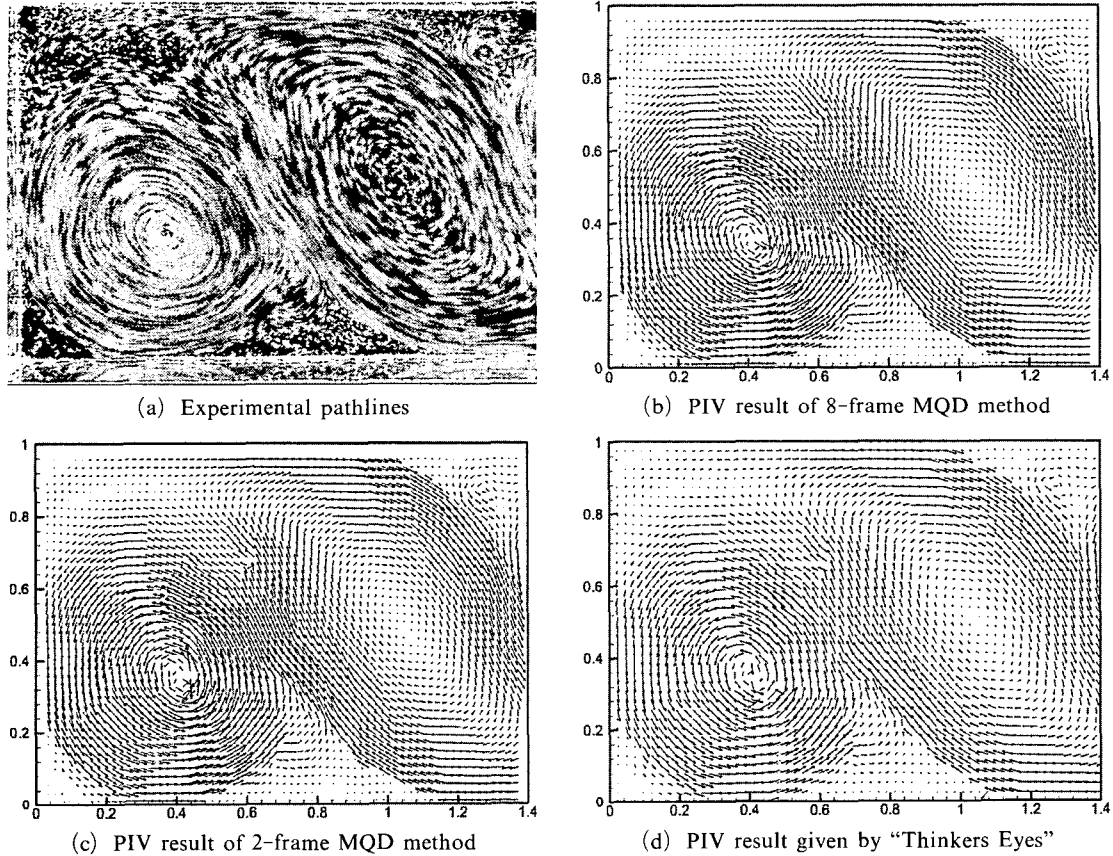


Fig. 12 Comparison of the PIV results for the spin up flows in a rectangular container given by the 8-frame MQD method (b), 2-frame MQD (c) and 2-frame c-c method (d) with $n_{sb}=15$ and $n_{pw}=25$. Also shown in (a) are pathlines made of 8 consecutive image-frames; $Re=26,180$, $\omega=0.64$

study on this flow has been given by Suh and Choi (2002). The container is located in a table which rotates with the angular velocity increasing smoothly (the modulation function being sinusoidal) from 0 to 0.6545 rad/s in 9.6s. The relative flow inside the container is visualized by light particles floated on the free surface and the particles' movement is recorded in a video camera corotating with the table. In this experimental set-up the Reynolds number is computed to be 26,180.

Figure 12 shows the results obtained by 8-frame MQD, 2-frame (simple) MQD and c-c methods for the velocity field 20s after start-up of the table's rotation. The pathlines made of 8 consecutive images are given in (a). We can see that the 8-frame MQD provides the best result,

whereas both the simple MQD and the commercial code yield some error vectors especially in the center of the counter-clockwise (cyclonic) vortex. In overall the simple MQD method and the commercial code are shown to result in almost the same level of accuracy.

Figure 13 shows the vorticity contours given by a direct numerical simulation in (a), the 8-frame MQD method in (b), the simple MQD method in (c) and the commercial code in (d). We can see that all the PIV results give contour patterns which is more irregular than the CFD result; the CFD result in (a) has been obtained for $Re=20,000$ which is slightly less than the experiment, but it is exhibited here as a standard pattern.

The CPU time needed in the computation of the vector field in the simple MQD method was

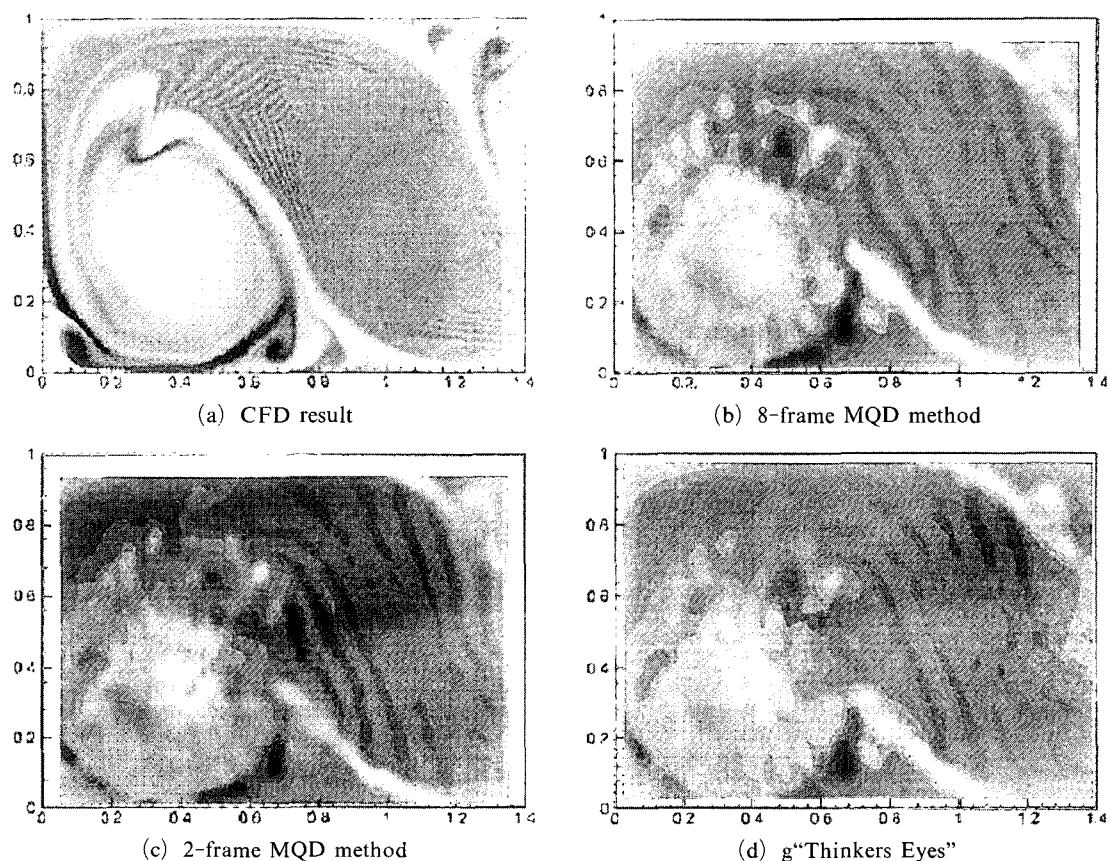


Fig. 13 Comparison of the vorticity contours for the same flow as Fig. 12 given by the 8-frame MQD method (b), 2-frame MQD method (c) and 2-frame *c-c* method (d). Also shown in (a) are the numerical result given by a CFD code for $Re=20,000$, $\omega=0.64$

1 min 10 s which is shorter the 1 min 30 s for the commercial code.

5. Conclusions

The conventional cross-correlation method is simple in usage and fast in operation, but it turns out that the method yields comparatively many error vectors. The normalized cross-correlation method developed to reduce the error vectors partially overcomes the defect but it has a serious drawback in that the algorithm becomes singular for a small interrogation-window size. The MQD method is free from these problems, and it is shown to be more economical than the conventional cross-correlation methods; for the same interrogation-window size, the MQD method is

twice faster than the normalized *c-c* method while the accuracy is almost in the same level.

The error vectors can of course be removed in the post-process of PIV not only in the conventional cross-correlation but in the proposed method as well; in this case the present method can enjoy additional benefit that the interrogation window size may be further decreased and small-scale flow structures relevant in turbulence can be better resolved.

The multi-frame MQD method presented in this paper for finding particles' displacements from a sequence of multiple images further reduce the error vectors. The error vectors caused by particles' entering and/or leaving the light sheet in the experiment are in fact reduced by constructing a new object function given by summing

all the individual object functions obtained for the sequence of image data. In this way the effect of particles' entering and/or leaving the visualization domain can be partially eliminated. However one must bear in mind that employing the multiple images in the PIV method can give rise to the time-averaging effect and therefore it should be used with care when, for instance, the representative time scale of the flow field is not sufficiently larger than the time interval between two neighboring flow images used in determining the velocity field with PIV.

Further study needed in association with the multi-frame MQD method includes speed-up of computation by employing FFT and further reduction of the error vectors by combining the multi-grid PIV method.

Acknowledgment

This work has been supported by grant No. R12-2002-058-01004-02003 from the Center for Advanced Net Shape Manufacturing and Clean Processes of the Korea Science and Engineering Foundation.

References

- Beebe, D. J., Adrian, R. J., Olsen, M. G., Stremmer, M. A., Aref, H. and Jo, B. H., 2001, "Passive Mixing in Microchannels," *Mec. Ind.*, Vol. 2, pp. 343~348.
- Chetelat, O., Yoon, S. Y. and Kim, K. C., 2001, "Design and Construction of a Miniature PIV (MPIV) System," *KSME Int. J.*, Vol. 15, No. 12, pp. 1775~1783.
- Gui, L. and Merzkirch, W., 1996, "A Method of Tracking Ensembles of Particle Images," *Exp. Fluids*, Vol. 21, pp. 465~468.
- Gui, L. and Merzkirch, W., 2000, "A Comparative Study of the MQD Method and Several Correlation-Based PIV Evaluation Algorithms," *Exp. Fluids*, Vol. 28, pp. 36~44.
- Lecerf, A., Renou, B., Allano, D., Boukhalfa, A. and Trinit, M., 1998, "Stereoscopic PIV: Validation and Application to an Isotropic Turbulent Flow," *Exp. Fluids*, Vol. 26, pp. 107~115.
- Liu, R. H., Stremmer, M. A., Sharp, K. V., Olsen, M. G., Santiago, J. G., Adrian, R. J., Aref, H. and Beebe, D. J., 2000, "Passive Mixing in a Three Dimensional Serpentine Microchannel," *J. MEMS*, Vol. 9, No. 2, pp. 190~197.
- Meinhart, C. D., Wereley, S. T. and Santiago, J. G., 1999, "PIV Measurements of a Microchannel Flow," *Exp. Fluids*, Vol. 27, pp. 414 ~ 419.
- Raffel, M., Willert, C. and Kompenhans, J., 1999, *Particle Image Velocimetry*, Springer-Verlag.
- Strook, A. D., Dertinger, S. K. W., Ajdari, A., Mezić, I., Stone, H. A. and Whitesides, G. M., 2002, "Chaotic Mixer for Microchannels," *Science*, Vol. 295, pp. 647~651.
- Suh, Y. K. and Choi, Y. H., 2002, "Study on Two-Dimensional Spin-up of Fluid in a Rectangular Container Using Ekman Pumping Models," *J. Fluid Mech.*, Vol. 458, pp. 103~132.